Article

The Spatial Pattern and Mechanism of Thermal Environment in Urban Blocks from the Perspective of Green Space Fractal

Yilu Gong [1] , **Xueming Li** [2], **He Liu** [2] **and Yu Li** [1,*]

1   School of Art and Design, Dalian Polytechnic University, Dalian 116034, China
2   School of Geography, Liaoning Normal University, Dalian 116029, China
*   Correspondence: liyu@dlpu.edu.cn

Abstract: Land resources in cities are limited, and the cost of green space construction is high. Compared with increasing the amount of green space, maximizing the cooling effect of limited green space has important theoretical and practical significance. Green fractal is a new innovative branch of urban fractal that uses a fractal index to quantify the green space structural index in studying the thermal environmental effect. Multi-source data, such as high-resolution remote sensing images, were used, and spatial regression models and inconsistency indices were applied to explore the spatial pattern of the urban thermal environment at the block scale, and the mechanism of green space fractal characteristics in terms of correlation and spatial heterogeneity, to assess the quality of green space development. This study shows the following: (1) In 2019, the land surface temperature in Dalian formed a spatial distribution structure of "high in the central region and low in the surrounding region" at the block scale, and the fractal indices of different green spaces show the spatial distribution structure of "dual-core" and "multi-core" spaces. (2) The driving direction and force of the fractal index of green space on the spatial pattern of land surface temperature differs. The influence of the green space structure index (grid and boundary dimensions) is greater than that of the quantity index (area and circumference), and the influence of the grid dimension is the most significant. (3) The spatial heterogeneity between the fractal index of block-scale green space and land surface temperature in Dalian is significant, showing a centralized and contiguous spatial pattern, with a trapezoidal structure decreasing from north to south. (4) The spatial adaptation between the fractal and thermal environments of green spaces can be evaluated using the inconsistency index. The development quality of green space can be divided into three types: advanced, relative coordination, and lagged green spaces. Finally, this study proposes specific suggestions for the development of block-scale green spaces and thermal environment management in Dalian City.

Keywords: urban green space; thermal environmental effects; multi-source data; fractal model

1. Introduction

Under the dual influence of urbanization and global climate change, the urban heat island effect is intensifying, which not only seriously affects the thermal comfort of the human body and the health of residents [1–4], but also has an important influence on urban ecological function and regional sustainable development [5,6]. As an important part of the urban ecosystem, the green space system has a variety of ecological functions that can effectively stabilize the urban ecological environment and improve the quality of the living environment [7]. Concurrently, the structural indicators of green space, such as green space form, structure, and spatial layout, also have a significant impact on the thermal environment. Urban land resources are limited, and greenspace construction costs are high. Compared with increasing green space quantity, optimizing the green space landscape pattern, improving the cooling function of green space per unit area, and maximizing the cooling effect of limited green space has important theoretical and practical significance [8–14].

The thermal environment effect on green spaces is the focus of urban thermal environment research. Scholars at home and abroad have conducted much research in different cities using different methods. Thermal environment research methods mainly include field observation [15], remote sensing technology [16], numerical simulation [17], human thermal comfort perception [18], and comprehensive use of a variety of methods to carry out research. Field observation is often used for small-scale green patches, and the effective measurement range is small and easily limited by external conditions; however, the data have the advantages of continuity and high accuracy [19,20]. Remote sensing technology can simultaneously acquire land surface temperature data over a wide range and usually studies the thermal environmental effects of green space systems based on urban and regional spatial scales [21]. The numerical simulation method has the characteristics of fast research speed, adjustable research scale, and adaptability to complex urban patterns; however, it needs to be combined with field observation methods, FLUENT, ENVI-met, and other software [22]. Zhang et al. used numerical simulations to study how the number and layout of trees and pavements affected the thermal environment [23]. Zhu et al. studied the human physiological thermal response in different green spaces of urban parks using questionnaire surveys and physiological parameter and microclimate measurements [24].

As the object of study, green patches can be divided into vegetation and landscape scales. Vegetation scale studies have mainly focused on the effects of vegetation species, communities, types, and structures on the cooling function and effect of green space from the perspectives of botany, ecology, landscape architecture, and other disciplines. Liu et al. found that different tree species exhibited significant differences in cooling, humidification, and discomfort reduction rates [25]. Zhang et al. studied the cooling and humidifying effects of multilayer vegetation communities with different canopy densities at different times of day [26]. Su et al. studied the relationship between the leaf area index and evapotranspiration of different vegetation types in different climate zones [27].

Landscape scale studies mainly focus on the discussion of green quantity and green space structural indices. The study of green quantity is the focus of study of the thermal environment of green spaces. Scholars have discussed the thermal environmental effects of green quantity indicators such as green space area and rate, green coverage rate, leaf area index, tree coverage rate, three-dimensional green quantity [28], and sky visibility [29]. In general, the cooling effect of green space is nonlinear, with an increase in green amount, and there may be an optimal green amount. Threshold is a key issue that cannot be avoided; for example, Zhang et al.'s research shows that the greenbelt area should be between 0.6 and 0.7 km^2, or the circumference should be between 4000 and 4500 m when the internal temperature is the lowest [30]. Pang et al. showed that there is an efficiency threshold (TVoE) of about 0.52 ha in waterless green areas of cities in cold regions of China, while there is no TVoE in green areas containing water [31]. The thermal environmental effect of the green space structural index points to the influence of morphological, structural, and spatial layout characteristics of green space patches on the green space itself and the overall landscape environmental temperature. At present, the main research methods are based on the statistical relationship between the green space landscape pattern index and temperature. The commonly used landscape pattern indices include patch number, mean patch area, patch density index, boundary density, maximum patch index, landscape shape index, evenness index, separation index, and convergence index [32–35].

Research on the thermal environmental effect and cooling mechanism of urban green space has gradually become a popular topic, shifting from focusing on the development of a green quantity index to focusing on the structural indicators of the green space system. However, the study still has the following problems: (1) Most of the research objects are single green patches (such as park green patches), and there are few studies on urban (regional)-scale green space systems. This is directly related to the difficulty and accuracy in green space and thermal environment data acquisition. High-resolution remote sensing images may provide better research conditions. (2) At the landscape scale, the research method was limited to the landscape pattern index. Different scholars choose different

research scales and indicators, thus, the research results are not highly comparable and integration with the practice of territorial spatial planning is insufficient. (3) In contrast to the convergence of green quantity research results, the impact of green space structural indicators on the thermal environment presents different or even opposite results in different studies. This is related to the differences in the climate background, urban structure, data resolution, and research and analysis methods in the study area; therefore, further research is required.

The marginal contribution of this study is as follows: (1) At the smallest scale of China's territorial space planning practice (urban block), this study explores how structural indicators influence the cooling effect of green space. Using high-resolution remote sensing image data, the precision of green space extraction and the accuracy of the measurement results are improved. Docking with the detailed control planning scale in urban planning enhances the practical significance of green space structural optimization. (2) From the perspective of fractal theory, the fractal index of green space is quantified as its structural index, which has theoretical innovation significance. The thermal environmental effects of the green quantity index (area and perimeter) and green space structural index (grid and boundary dimensions) were compared under the same environmental conditions. (3) The inconsistency index was improved to evaluate the spatial matching relationship between the fractal and thermal environment of green space to evaluate the spatial heterogeneity of its development quality. This study is in the stage of basic theory and application of basic research, and its theoretical significance is more prominent.

In this study, GF1 and Landsat8 OLI/TIRS remote sensing image data were used as data sources. Supervised classification and atmospheric correction were applied to process the data, and green space and surface temperature data were extracted. Combined with the green space fractal model, a spatial regression analysis and inconsistency index analysis of the influence mechanism of urban green space fractal characteristics on the thermal environment is revealed. The quality of green space development at the block scale was evaluated from the perspective of cooling, and specific suggestions and optimization countermeasures are proposed for green space management and thermal environmental improvement.

2. Study Area and Data Sources

2.1. Study Area Overview

The downtown area of Dalian is south of Liaodong Peninsula. As an important economic, trade, and port city in the eastern coastal area of China, it includes four administrative regions, Zhongshan, Xigang, Shahekou, and Ganjingzi Districts, with a total area of 550.27 km^2. At the end of 2019, the registered population in the downtown area of Dalian was 2,111,300 (Figure 1).

The terrain of Dalian is mainly mountainous and hilly, supplemented by plains and lowlands. It is surrounded by the sea on three sides and has a transitional maritime climate. The Yellow Sea coast has a warm and humid continental monsoon climate, whereas the Bohai Sea coast has a warm and sub-humid continental monsoon climate. The annual extreme maximum temperature and annual minimum temperature in Dalian are 35.8 °C and −29.3 °C, respectively. The daily temperature range shows a decreasing trend from north to south, and the annual temperature range is between 28.7 °C and 31.8 °C. Since the 1990s, the urban social and economic development level of Dalian has increased rapidly, the building density and floor area ratio of the urban central area have been steadily increasing, and the intensity of human settlements has been relatively high. Compared with the surrounding areas, the urban center of Dalian has a significant heat island effect [36,37]. In addition, Dalian attaches great importance to urban ecological environmental development and urban green space planning and construction [38]. In 2019, the forest coverage rate of Dalian was 41.5% and the forest greening rate was 50%. In summary, the study area has rich vegetation types, mature urban green space development, a significant heat island effect, and prominent thermal environmental problems, which are representative and typical.

The alleviation of the heat island effect and solving the problems of the urban thermal environment have become key issues hindering the urban development of Dalian City.
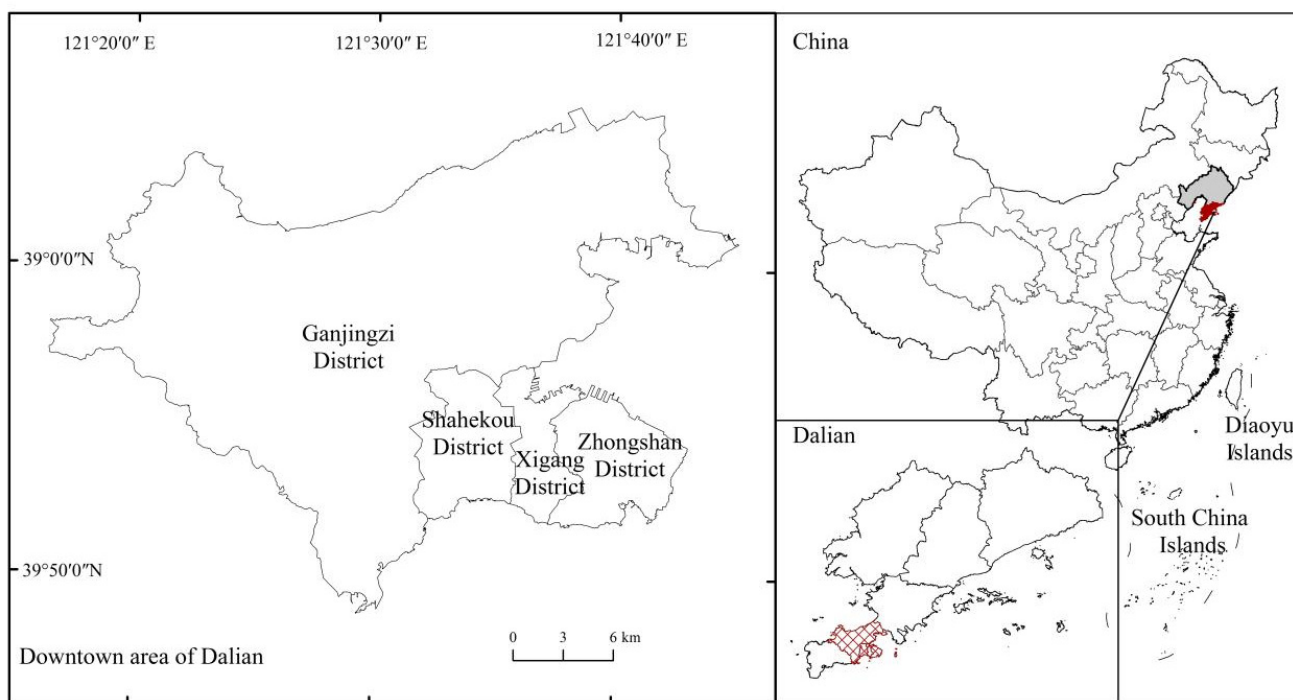

Figure 1. Study area.

2.2. Data Sources and Processing

The research data in this study are comprised of three main parts. First, high-resolution remote sensing image data were used to extract green space information, mainly through the remote sensing classification method combining maximum likelihood supervision classification and visual interpretation to extract green space information. Secondly, Landsat 8 OLI/TIRS data were used for land surface temperature (LST) inversion as an indicator of the land surface thermal environment. ENVI5.3 software was used for coordinate system definition, geometric correction, and cutting of image datasets. Third, Dalian block zoning data were obtained from the control management unit provided by the Dalian Natural Resources Bureau. The control management unit is the smallest management unit in urban planning, construction, and implementation. Therefore, the block management unit proposed in this study has the same spatial division scope and attributes as actual urban planning and construction implementation (Figure 2).

The surface temperature reflects the influence of human activity on the environmental temperature more than that of the air temperature; however, the process of extracting and calculating the surface temperature is more complicated. To determine a more scientific research year, a preliminary analysis was conducted using the air temperature data. By referring to the historical data of the monthly average temperature of Dalian City from 2011 to 2021 in the Statistical Yearbook of Dalian City, it was determined that the annual maximum temperature occurred from June to August, and the monthly average temperature was between 19.4 °C and 27 °C. The lowest temperature in June 2012 was 19.4 °C, and the highest temperature in August 2019 was 27 °C. Additionally, the average temperature from June to August was calculated, which showed an overall trend of initially increasing and then decreasing, reaching the highest values in 2018 and 2019, with an average temperature of 24.3 °C. Therefore, it is preliminarily judged that June–August 2019 is of research significance and value.
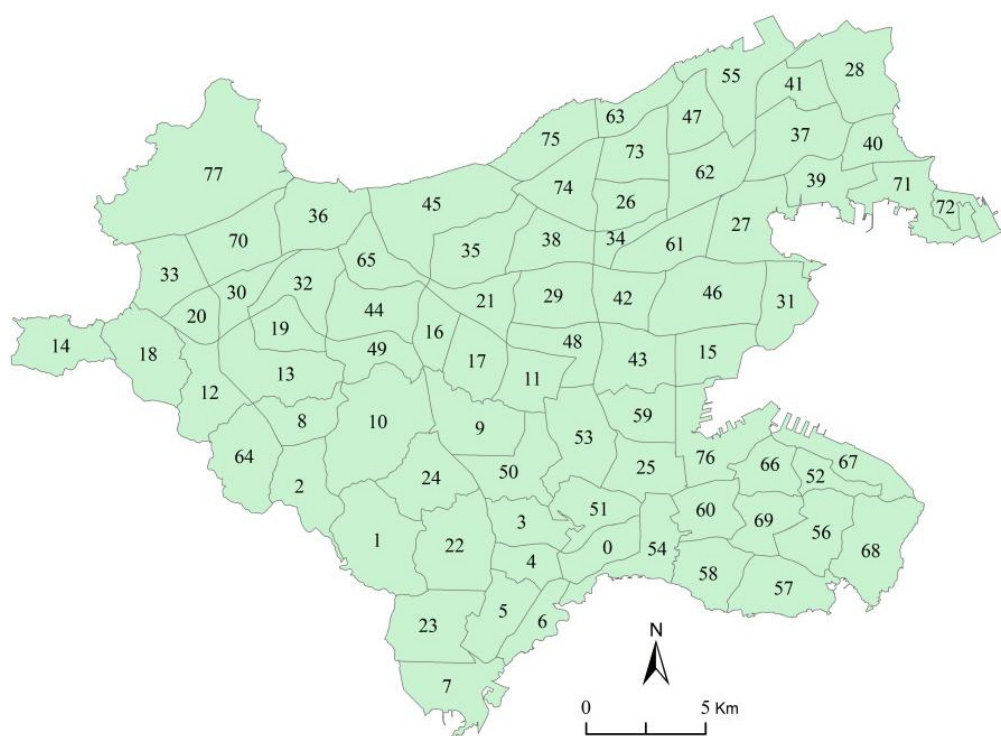
Figure 2. Location and serial number of the 78 blocks in Dalian.

To ensure the scientific nature of the research, green space and surface temperature data of the same month should be used. Owing to the limitation, compatibility, and errors in data acquisition, data from June 2019 were selected for further analysis. GF1 data from June were selected to obtain green space information, and Landsat-8 data from June were used to obtain LST information. The coverage time of the acquired remote sensing image was approximately 12:00 noon, the solar altitude was the highest, the building shadow and interference on the green space extraction was minimal, and the data error could be reduced. Taking Block 15 as an example, the green space information extracted using remote sensing images is shown in Figure 3. The accuracy of the extracted green space can reach approximately 1.5–2 m. Compared with the Landsat data, the extracted green space information is more abundant. Large areas of natural and complex artificial green space can be clearly seen, among which the artificial green space shows an urban traffic green belt, industrial shelterbelt, inter-residential green space in the residential area, grass in the school playground, various types of park green space, and so on. The data sources and processing are listed in Table 1.

Table 1. Data source and processing.

Data Name	Access Time	Data Description	Data Sources	Data Processing
GF1	13 June 2019	Spatial resolution 2 m, the revisit cycle is 4 days, covering 41 day, 3 bands	Dalian Natural Resources Bureau	A remote sensing classification method combining maximum likelihood supervised classification and visual interpretation was used to extract green space information. Accuracy verification—the verification points were selected from the corresponding landscape type map and Google Earth image map of the corresponding year, and the classification confusion matrix was calculated based on the classification results. The Ground Truth (Green space) was 96.01%, and the Kappa Coefficient was 0.848.

| Data Name	Access Time	Data Description	Data Sources	Data Processing
Landsat-8 OLI/TIRS	25 June 2019	Spatial resolution 30 m, good without clouds, image band number 120,033	http://glovis.usgs.gov/ accessed on 25 June 2019	The LST was retrieved by atmospheric correction and ENVI software.
Block zoning data	2019	Including main roads, secondary roads, and roads of	Equivalent to the control and regulation management unit	The 78 blocks were numbered for study convenience and named from 0 to 77.
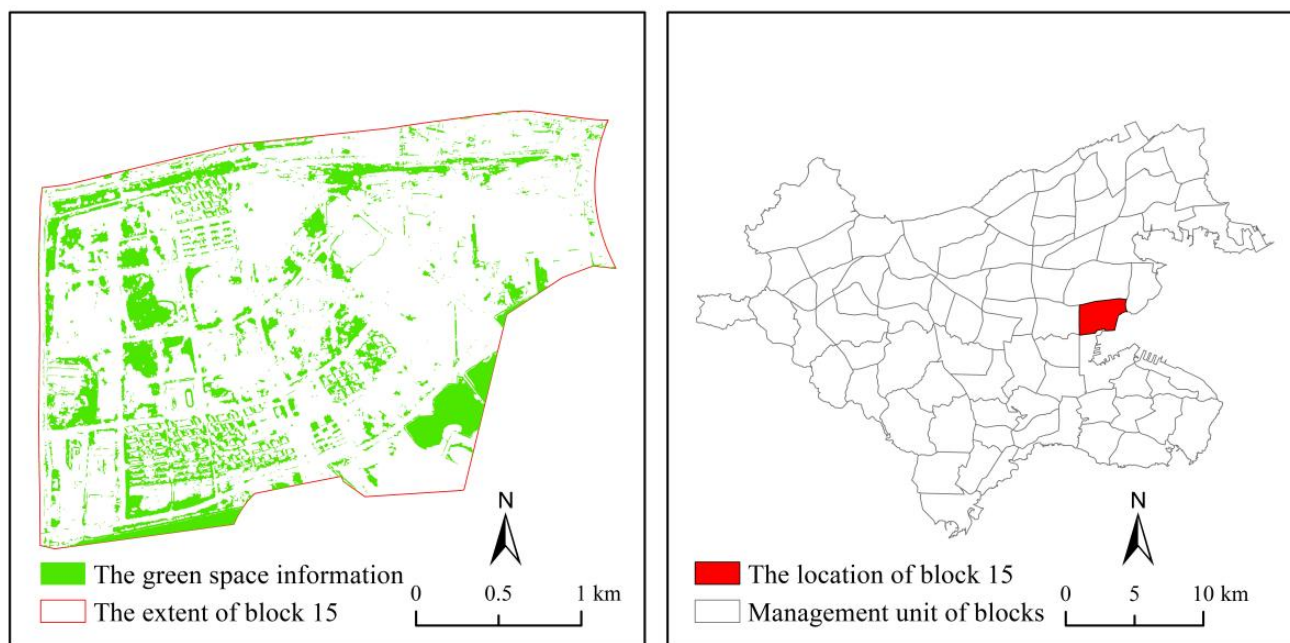
Figure 3. The green space information extracted from remote sensing images.

3. Methodology

3.1. Surface Temperature Inversion Algorithm

The inversion of LST in this study adopts the atmospheric correction method (also known as "radiative conduction equation method"), and ENVI software is used to process Landsat data and inversion of LST. The steps of the LST inversion are as follows [39]:

(1) Radiometric correction

The radiometric calibration tool under radiometric correction of ENVI software was used to conduct radiometric calibration of the multispectral and thermal infrared bands of Landsat 8 OLI/TRIS remote sensing images. In this manner, the radiation error caused by the sensor's own characteristics, terrain, and atmosphere can be eliminated, and the noise in the image can be removed.

(2) Calculation of normalized difference vegetation index (*NDVI*)

$$Pv = [(NDVI - NDVISoil)/(NDVIVeg - NEVISoil)] \tag{1}$$

where *NDVI* represents the normalized difference vegetation index, *NDVISoil* represents the *NDVI* value of bare soil or non-vegetation-covered areas, and *NDVIVeg* represents the *NDVI* value of pixels completely covered by vegetation. Here, the simplified FVC model in *ENVI* was used to calculate the *NDVI* value, and the FVC image was obtained via band calculation.

(3) Calculation of surface emissivity

Sobrino believed that the land surface is composed of vegetation and bare land. He used *NDVI* to classify the land surface and the *NDVI* threshold method to calculate the specific emissivity of the land surface. On this basis, a mixed model method was used to calculate the surface emissivity [40].

When *NDVI* < 0.2, the land surface was completely covered by bare land and the surface emissivity value was 0.973.

When $0.2 \leq NDVI \leq 0.5$, the land surface includes vegetation and bare land. Here, the surface-specific emissivity is as follows:

$$\varepsilon = 0.0004Pv + 0.986 \tag{2}$$

When *NDVI* > 0.5, the land surface was completely covered by vegetation, and the surface emissivity value was 0.986, which is the typical emissivity value of vegetation, where P_v represents the vegetation coverage.

(4) Calculation of blackbody radiance

$$B(T_s) = \frac{I - L \uparrow - \tau \times (1 - \varepsilon) \times L \downarrow}{\tau \times \varepsilon} \tag{3}$$

where $B(T_s)$ r represents the blackbody radiation brightness and I represents the thermal radiation intensity, which can be calculated according to the DN value of the thermal infrared band and is the known value [41]. $L\uparrow$ and $L\downarrow$ are the upward and downward heat radiation intensities of the atmosphere, respectively, and τ is the transmittance of the atmosphere in the thermal infrared band.

On NASA's website (http://atmcorr.gsfc.nasa.gov accessed on 25 June 2019), the center of shadow time, latitude and longitude, and other relevant parameters are entered, and it is concluded that the atmospheric profile information is as follows: (1) Atmospheric transmittance τ: 0.78. (2) Atmospheric upward radiation brightness $L\uparrow$: 1.81 W/(m^2·sr·μm). (3) Atmospheric downward radiation luminance $L\downarrow$: 2.96 W/(m^2·sr·μm).

(5) Calculation of surface temperature

$$T = \frac{K_2}{ln[1 + K_1 / B(T_s)]} - 273 \tag{4}$$

where *T* represents the land surface temperature, $B(T_s)$ represents the blackbody radiation brightness, K_1 is 774.8853 W/(m^2·sr·μm), and K_2 is 1321.0789 K in the Landsat 8 OLI/TRIS remote sensing images. To eliminate spatio-temporal differences among remote sensing images, the surface temperature was normalized using range normalization.

3.2. Green Space Fractal Model

The fractal concept of green space originates from urban analysis, and is a new branch separated from urban fractal. This refers to the analysis of the morphological and structural characteristics of green spaces using fractal theory [42]. This study mainly explores the morphological and structural characteristics of green spaces from the dual aspects of grid and boundary dimensions.

(1) Grid dimension

The grid dimension is primarily determined using the box counting method to measure urban land, among which box counting is the most basic method for measuring fractal curves by the covering method, which can not only be used to judge fractal features but also to calculate fractal dimensions [43]. The calculation process of the grid dimension is as follows. First, the geographical objects, such as urban green space, are covered by a rectangular area; the side length of the rectangle *r* is *L*, and only a rectangular area is occupied by geographical objects, which is not empty, giving grid number *N(L)* = 1. The rectangular area is sectioned into four small rectangles of equal sizes. One side of the small rectangle *r* is *L/2*, and the number of non-empty grids is *N(L/2)*. The small rectangular

area is further divided, and the large rectangular area is divided into 16 equal parts. The side lengths *r* of the small rectangle are $L/4$ and $L/2^2$, and the number of non-empty grids is $N(L/2^n)$. If the urban green space has fractal characteristics, it can be shown according to fractal theory [44]:

$$N(\frac{L}{2^n}) = 2^{-D} N(\frac{1}{2^{n+1}})$$ (5)

Conforming to the negative power function,

$$N(r) \propto r^{-D}$$ (6)

If the scaling invariance defined in the above equation is satisfied, *D* is the fractal dimension. If there is a negative power exponential relationship between grid scale *r* and the number of non-empty grids $N(r)$, it can be judged that the urban green space has fractal characteristics. The value range of the grid dimension *D* for urban fractals was [0, 2]. In terms of geographical geometry, the grid dimension represents the filling degree of a certain urban land type and equilibrium land-use type. The larger its value, the more significant the equilibrium characteristic of the urban land spatial distribution, while the smaller its value, the more obvious the concentration characteristic of the urban land spatial distribution. In this study, Block 15 was used as an example to draw a double logarithmic diagram of the green space grid dimension. As shown in Figure 4, the goodness of fit coefficient R^2 is 0.9979, which indicates that the green space grid dimension of block 15 in Dalian City has fractal characteristics.
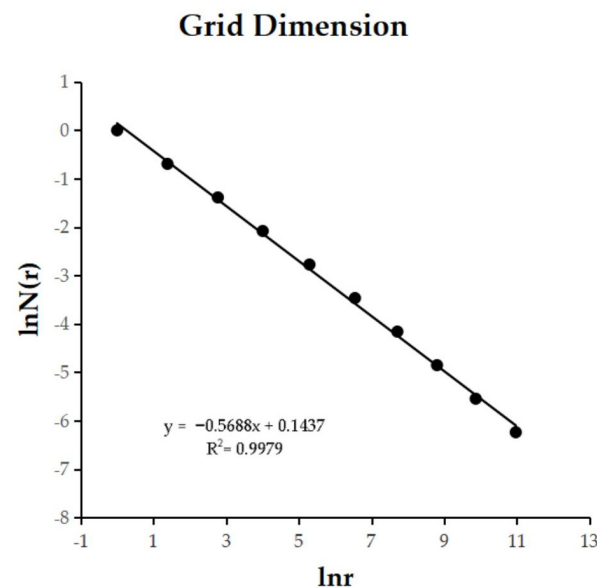

Figure 4. Grid dimension double logarithm diagram of green space in Block 15.

(2)   Boundary dimension

There are two ways to define the boundary dimension—based on the circumference–scale and area–perimeter relationships. The boundary dimension defined by the circumference–scale relationship can be realized by the box counting method, and the length *r* of the rectangular side and the number of non-empty grids $N(r)$ covering the boundary can be obtained according to fractal theory [45]:

$$\ln N(r) = -D \ln r + C$$ (7)

where *C* represents an undetermined constant and *D* represents the boundary dimension. As shown in Figure 5, the goodness of fit coefficient R^2 dimension is 0.9949, which indi-

cates that the boundary dimension of green space in block 15 of Dalian City has fractal characteristics based on the perimeter scale.
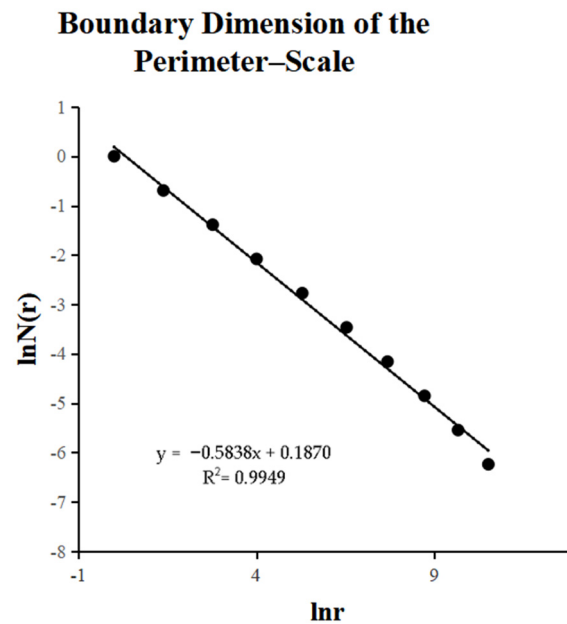

Figure 5. Bilogarithm diagram of boundary dimension estimated by circumference–scale model for Block 15.

Based on the boundary dimension defined by the area–perimeter relationship, the main research premise assumes that a certain city land-use type is *a* closed area, with areas *A* and *P*. We assume that the boundary of this area is a fractal line and is represented by dimension *D*. Then, according to the geometric measurement relationship, we can obtain the following:

$$A = kP^{\frac{2}{D}} \tag{8}$$

where *k* represents a constant that needs to be determined. The double logarithmic transformation of the boundary dimension defined by the perimeter–scale relationship can be obtained as follows:

$$\log A = \frac{2}{D} \log P + C \tag{9}$$

The fractal dimension was estimated using the box-counting method. The number of non-empty grids $N(r)$ covering the boundary and the number of non-empty grids $M(r)$ covering the area is as follows:

$$\ln N(r) = \frac{2}{D} \ln M(r) + C \tag{10}$$

The boundary dimension defined by the perimeter–scale relationship can only reflect the complexity of the urban green space boundary. The larger its value, the more complex the boundary of urban green space will be. For the urban form, the value of *D* ranges from 0 to 2. The boundary dimension defined by the area–perimeter relationship can reflect more information about the distribution of urban land-use to a certain extent. It can show both the complexity of the urban land-use boundary, the fragmentation degree of urban land-use, and the degree of stability of its land-use structure. Theoretically, for the overall urban land-use structure, *D* is between 1 and 2. When *D* < 1.50, the urban green space form is relatively simple; when *D* = 1.50, the urban green space form is in a random state, similar to Brownian motion, and when *D* > 1.5, the urban land-use structure is relatively complex. As shown in Figure 6, the goodness of fit coefficient R^2 dimension is 0.9992, which

indicates that the boundary dimension of the green space of block 15 in Dalian City has fractal characteristics based on the perimeter area.
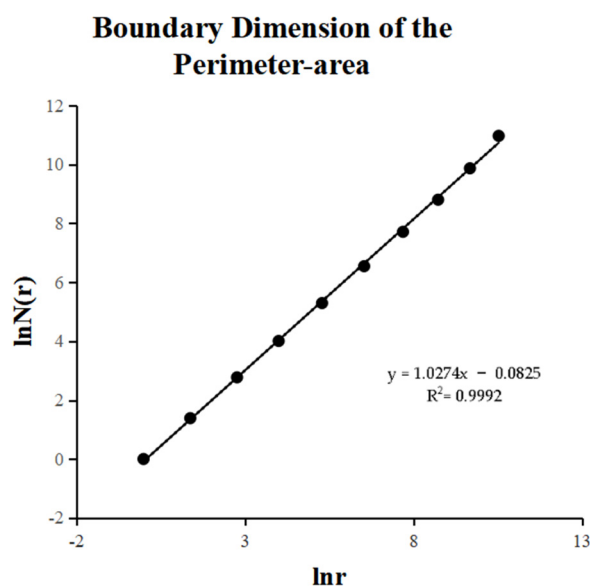

Figure 6. Bilogarithmic graph of boundary dimension estimated by circumference–area model for Block 15.

3.3. Spatial Regression Analysis

This study used GeoDa 1.6 software and a spatial autoregression model to perform regression analysis on LST and the green space landscape index. Commonly used spatial autoregressive models include the spatial lag model (SLM) and spatial error model (SEM). which are calculated as follows [46].

$$\text{Spatial lag model (SLM): } Y = \rho W y + X\beta + \varepsilon \tag{11}$$

$$\text{Spatial error model (SEM): } Y = X\beta + \mu \tag{12}$$

$$\mu = \lambda W \mu + \varepsilon \tag{13}$$

where Y represents the dependent variable (LST), X represents the independent variable (various green landscape indices), β represents the regression coefficient, μ and ε are random error terms, W represents the spatial adjacency weight matrix, ρ represents the regression coefficient of the spatial lag term, and λ represents the regression coefficient of the spatial residual term.

In the model index selection, the dependent variable was the urban thermal environmental index. To compare the influence of the green quality and green space structural indices on the thermal environment, two indices were added as explanatory variables. The final explanatory variables were the green space boundary dimension (X1) estimated by the perimeter–scale model, green space boundary dimension (X2) estimated by the perimeter–area model, green space grid dimension (X3), green space area (X4), and green space perimeter (X5). The fractal index of green space is a structural index that reflects the green space area and perimeter after calculation using the green space area and green space perimeter data. The green space area (X4) can be compared with the grid dimension (X3), and the green space perimeter (X5) can be compared with the boundary dimension (X1) estimated using the girth–scale model.

3.4. Inconsistency Index

The matching relationship (spatial distribution inconsistency) between the urban green space fractal characteristics and LST was quantitatively analyzed using the inconsistency index. The calculation formula is as follows [47].

$$RT_i = T_i / \sum T_i \tag{14}$$

$$RG_i = G_i / \sum G_i \tag{15}$$

$$I_i = RT_i / RG_i \tag{16}$$

where T_i and G_i represent the mean surface temperature of the *i*th grid and the fractal dimension of green space, respectively; $\sum T_i$ and $\sum G_i$ are the cumulative mean temperature and fractal dimension of the study area, respectively; RT_i represents the proportion of the mean surface temperature of the *i*th grid in the cumulative mean temperature of the study area; and RG_i represents the proportion of the fractal dimension of the *i*th grid in the sum of the studied discriminative dimensions. The higher the values of RT_i and RG_i, the higher the clustering degree of the grid to LST and the green space fractal dimension. The inconsistency index, I_i, is the ratio of the two agglomeration indices. The closer the value is to 1, the more similar the change trend of the two agglomeration indices, and there is better synergy (consistency) between them. The more the absolute value deviates from 1, the less coordinated the spatial distribution of the two agglomeration indices.

As the city is a constantly changing system with complex characteristics, there are few cases where the inconsistency index is 1; therefore, the results of the inconsistency index calculation are divided into three types considering a dynamic error of $\pm 5\%$. When $I_i \leq 0.95$, the fractal agglomeration of green space is ahead of the surface temperature agglomeration; that is, green space is the leading type. When $0.95 < I_i < 1.05$, it is the coordination between green space fractal and LST agglomeration, that is, the relative coordination type. When $I_i \geq 1.05$, the fractal agglomeration of green space lags behind the agglomeration of LST; that is, it is a backward type of green space.

4. Result Analysis

4.1. Spatial Pattern of the Urban Thermal Environment

The thermal environmental effect in Dalian is notable, and there are obvious spatial differences among the different areas. Using the natural breakpoint method in ArcGIS, the average temperature of the Earth's surface was divided into five low-temperature grades in Dalian—low temperature, sub-low temperature, medium temperature, sub-high temperature, and high temperature—to directly show the average surface temperature distribution in 2019 for each district block in Dalian (Figure 7). Figure 7 shows a pattern of gradual increase from the coastal low-latitude area to the inland high-latitude area, indicating a spatial distribution structure that is "high in the central area and low in the surrounding area." Among the blocks, the high-temperature area forms a distribution pattern of continuous agglomeration in central Dalian. The highest surface temperature of the blocks in Dalian was 39.37 °C, the lowest was 28.04 °C, and the average was 34.25 °C. The surface temperatures of the 47 blocks were higher than the average surface temperature of the main urban area of Dalian, accounting for 60.26% of the total number of blocks (Figure 8). To some extent, this shows that the surface temperature of the blocks in Dalian is relatively high, and the urban thermal environmental effect is obvious.
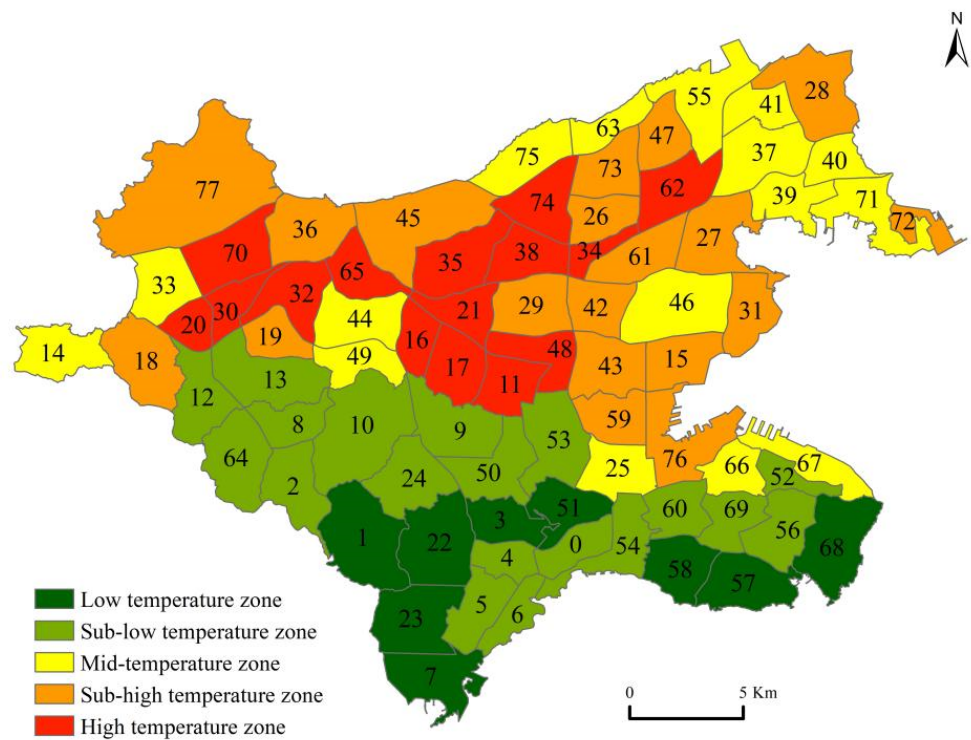
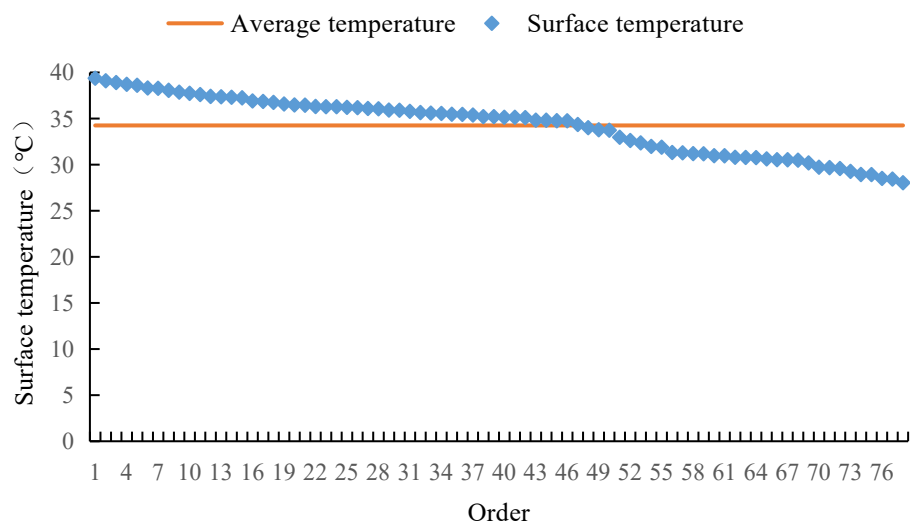**Figure 7.** Spatial distribution of surface temperature of blocks in Dalian.

Figure 8. Position order-scale of the surface temperature.

Overall, the proportion of LST at all levels in Dalian was uniform. The proportions of low temperature, sub-low temperature, medium temperature, sub-high temperature area, and high temperature areas were 11.54%, 24.36%, 20.51%, 24.36%, and 19.23%, respectively, showing that sub-high temperature and sub-low temperature areas were the main areas overall. In addition, the areas with high LST were mainly concentrated in Ganjingzi District at the edge of the downtown area, which differs from the spatial layout of the general urban heat island effect. The main reasons for the difference are as follows. First, the thermal environment index of this study is expressed by the surface temperature, which differs from the air temperature in the region. Second, there are many industrial enterprises in the area along the edge of Dalian, and the heat released by industrial production and other activity has a direct impact on surface temperature. Third, the environmental quality of

green space in the area along the edge of Dalian is low, and the effect of green space on alleviating the thermal environment is not obvious.

4.2. Spatial Pattern of Urban Green Space Fractal Characteristics

4.2.1. Grid Dimension Analysis

The grid dimension of green space in Dalian presents a "double core" spatial distribution structure with No. 34 and No. 72, with obvious local differences (Figure 9). Among them, the concept of "dual core" is mainly derived from the theory of urban spatial structure, which refers to the distribution structure of two centers in the inner space of a certain geographical phenomenon [48]. In Dalian, there were 13 blocks with values between 0.5172 and 0.5330. The green space grid dimension of 17 blocks was between 0.5330 and 0.5477, and there were 28 blocks with values between 0.5477 and 0.5659. There were 18 blocks with values between 0.5659 and 0.6017, and two blocks with values between 0.6017 and 0.6548, which shows that the grid dimension of Dalian green space has non-equilibrium characteristics.
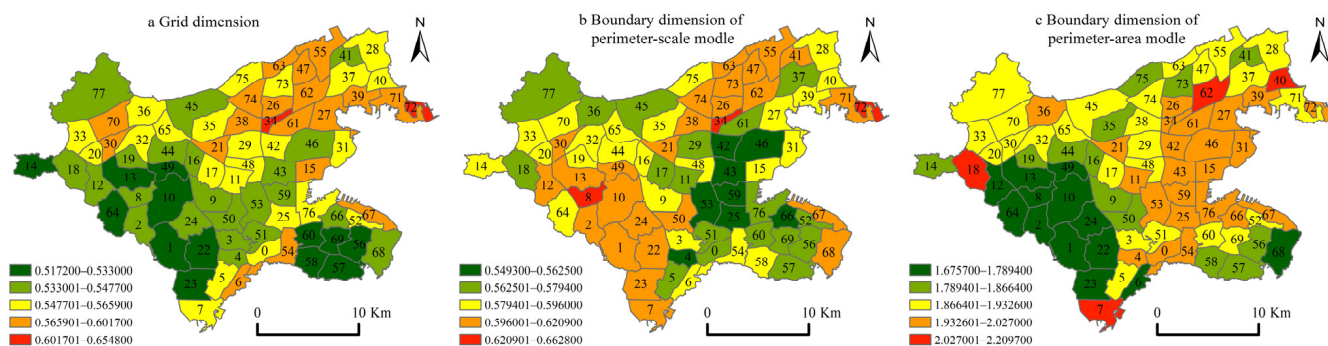

Figure 9. Spatial distribution of green space fractal characteristics of 78 blocks in Dalian.

The grid dimension of the green space in 78 blocks of Dalian was between 0.5172 and 0.6548, and the fitted R^2 was greater than 0.996, showing that the fractal characteristics of the green space grid dimension at the block scale are obvious. The grid dimension represents the balance of the green space structure. The block with the highest grid dimension was No. 34, at 0.6548, indicating that this block had the highest balance of green space.

4.2.2. Boundary Dimension Analysis of the Perimeter–Scale Model

Based on the circumference–scale model, the green space boundary dimension in Dalian City presents a multi-core spatial distribution pattern centered on the blocks No. 8, 34, and 72, with obvious spatial differences (Figure 9). Similar to the concept of "dual core," the concept of "multi core" refers to the distribution structure of multiple centers in the inner space of a certain geographical phenomenon [48]. There were 8 blocks in Dalian with green space boundary dimension values ranging from 0.5493 to 0.5625, 18 blocks with values ranging from 0.5625 to 0.5794, and 24 blocks with values ranging from 0.5794 to 0.5960. There were 25 blocks with values ranging from 0.5960 to 0.6209, and 3 with values ranging from 0.6209 to 0.6628, showing that the complexity of green space boundary forms in Dalian was mainly concentrated between 0.5960 and 0.6209.

Based on the perimeter–scale model, the green space boundary dimension of each block in Dalian ranged from 0.5493 to 0.6628, and the highest value was 0.6628 in the No. 34 block. The perimeter–scale model represents the complexity of the green space boundary morphology, showing that the green space morphology in block 34 was the most complex and had the highest value in the grid dimension, which is notable.

4.2.3. Boundary Dimension Analysis of the Perimeter–Area Model

Based on the perimeter–area model, the boundary dimension of green space in Dalian showed a "multi-core" spatial distribution structure with the block of No. 7, 18, 40, and 62

as the center, and some areas showed a continuous centralized distribution trend (Figure 9). There were 13 blocks with values between 1.6757 and 1.7894, 13 blocks with values between 1.7894 and 1.8664, and 25 blocks with values between 1.8664 and 1.9326. There were 23 blocks with values between 1.9326 and 2.0270, and 4 blocks with values between 2.0270 and 2.2097.

The boundary dimensions of 78 blocks in Dalian were between 1.6757 and 2.2097, among which the boundary dimensions of No. 40, 18, 62, and 7 were greater than 2. For urban fractals, the boundary dimension calculated by the circumference-area model was between 1 and 2, and this was the first time that the boundary dimension exceeded 2 at the block scale in the fractal dimension of the urban green space system. The boundary dimension estimated by the perimeter–area model represents the fragmentation and instability of the green space structure, which shows that the green space structure is more complex and unstable at the block scale.

4.3. Correlation Analysis between Urban Thermal Environment and Green Space Fractal Characteristics

When exploring the mechanism of the fractal index of urban green spaces on the thermal environment at a block scale, it is necessary to consider the influence of their spatial correlation. This is expected to determine the most significant factors affecting the urban thermal environment at the block scale and advance effective measures to maximize the cooling effect of green space.

The spatial autoregressive model was used to calculate the action mechanism of the urban green space fractal index on the urban thermal environment, and the regression results are shown in Table 2. As can be seen from Table 2, the residual Moran's I was 6.623, which shows that the residual of the least-squares method has obvious spatial dependence through the 1% significance level test. The interaction and mutual influence of different fractal indices of urban green spaces promotes the formation of a spatial pattern of an urban thermal environment. To further explore the mechanism of the fractal index of urban green space systems in urban thermal environments, a suitable spatial autoregressive model should be selected for further analysis. By comparing the LMLAG, LMERR, and other related indicators, it was noted that the SEM fit was better than that of the SLM. To some extent, it reflects the error impact of the regional thermal environment by the neighboring region thermal environment, which is stronger than that of the degree of spatial spillover.

Table 2. Estimation results of the effect of urban green space fractal indicators on urban thermal environment.

Variables	OLS	SLM	SEM
X1	−33.933	−32.293	−20.945
X2	−4.518	−4.401	1.985
X3	73.106 ***	70.551 ***	39.669 ***
X4	−0.000	−0.000	−0.000
X5	−0.000	−0.000	−0.000
ρ	-	0.055	-
λ	-	-	0.841 ***
R2	0.405	0.418	0.851
Log L	−178.725	9177.919	−143.047
AIC	369.45	369.838	298.093
SC	383.59	386.335	312.233
Moran's *I* (error)	6.623 ***	-	-
LMLAG	-	1.325	-
R-LMLAG	-	38.346 ***	-
LMERR	-	-	37.999 ***
R-LMERR	-	-	39.672 ***

Note: *** indicate significant at the 1% level.

As shown in Table 2, the error coefficient (λ) of the SEM was 0.841, and the 1% significance level test showed that there was an obvious spatial effect on the spatial distribution of urban LST in Dalian. According to the regression results of the SEM, the influence coefficient of area (X4) and perimeter (X5) on LST was 0, indicating that the green quality index had almost no influence on LST at the block scale, and the cooling effect of green space mainly came from the comprehensive effect of the green space structural index.

At the block scale, the influence coefficient of the spatial difference pattern based on the perimeter–scale model was −20.945. Although the significance test failed, the X1 effect coefficient was significantly higher than that of X2. This shows that the complexity of the urban green space boundary line at the block scale is greater than that of the green space structure. X1 was negatively correlated with the spatial difference in the surface temperature; therefore, the higher the complexity of the green space boundary line, the lower the surface temperature, and the greater the cooling effect of the green space.

The influence coefficient of the urban green space boundary dimension estimated based on the perimeter–area model of the spatial difference pattern of LST was 1.985, which did not pass the significance test. The coefficient of X2 was much lower than that of X1 and X3, showing that the fragmentation degree of the urban green space structure has a very low influence on LST at the block scale and can be ignored. However, judging from the direction of influence, the boundary dimension of the next-week length-area model at the block scale is positively correlated with the spatial difference in LST. The higher the fragmentation of green space at the block scale, the higher the surface temperature, and the lower the cooling effect of green space.

The influence coefficient of the urban green space grid dimension on the spatial difference pattern of LST was 39.669, which passed the 1% significance level test, and the coefficient of X3 was the highest, showing that the balance of urban green space structure has the largest and most significant influence on LST at the block scale. There was a significant positive correlation between the green space grid dimensions and the spatial difference in LST at the block scale. The higher the green space equilibrium, the higher the LST, and the weaker the effect of green space in alleviating the thermal environment.

4.4. Analysis of the Inconsistency between the Urban Thermal Environment and the Fractal Characteristics of Green Spaces

To evaluate the development quality of green space in the 78 blocks of the study area, the inconsistency index method was used to calculate the spatial matching relationship between the fractal index of green space and the LST. The correlation analysis in this study showed that the green space grid dimension had the greatest influence on the thermal environmental effect of green space fractal characteristics at the block scale, and other indicators failed the significance test. Therefore, this section only discusses the spatial heterogeneity of the green space grid dimensions and LST. Through the improvement of the inconsistency index model, the calculated results of the inconsistency index were visualized using ArcGIS software, as shown in Figure 10.

The spatial agglomeration characteristics of the inconsistency index between the green space grid dimension and the LST of the block in Dalian are significant, which basically presents the spatial pattern of concentrated contiguous distribution and roughly shows a trapezoidal structure decreasing from north to south. In terms of the number of blocks, the agglomeration green space grid dimension of 28.21% of blocks is ahead of the agglomeration surface temperature, which belongs to the "green space leading type." The cooling effect of green space in this type of block is poor, and the quality of green space development is low. These blocks were concentrated in the northwest of Ganjingzi District. The agglomeration degree of the green space grid dimension of 41.02% of the blocks is similar to the agglomeration LST, which is in the "relatively coordinated" development stage. The development quality of green space in this type of block is relatively coordinated with the cooling effect. These blocks are distributed in northeastern Ganjingzi District and in the middle of the study area. The agglomeration green space grid dimension of 30.77%

of blocks lags the agglomeration LST, which belongs to the "green space lag type." This type of block has a good cooling effect and high green space development quality, and these blocks are distributed in the south of the study area.
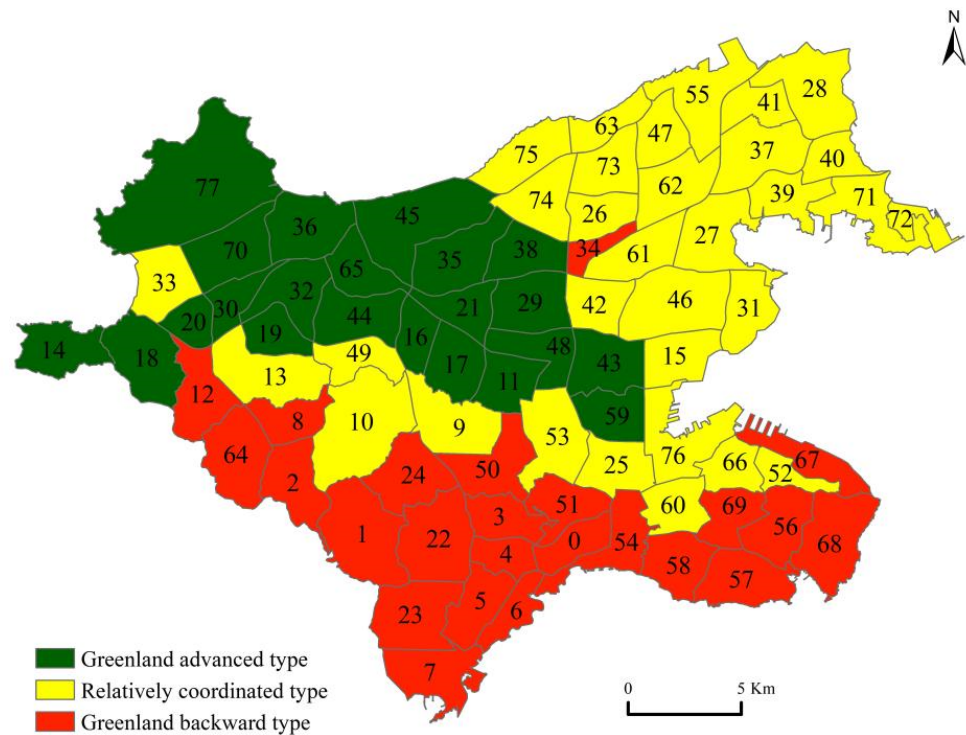

Figure 10. Spatial distribution of green space grid dimension and surface temperature inconsistency index of 78 blocks in Dalian.

5. Discussion

5.1. Governance Suggestions

Related studies have determined the cooling effect of green indicators, and this study further determined the cooling effect of the green space area structural index (grid dimension). The block scale is the basic unit to carry out territorial space planning, which has more practical significance. To improve the thermal environmental effect of urban green space at the block scale, the following relevant governance suggestions are proposed.

The thermal environment of Dalian in 2019 showed a gradual increase from low-latitude coastal areas to high-latitude inland areas, forming a spatial distribution structure of "high in the central and northern regions, low in the surrounding regions". There were significant spatial differences in the thermal environmental effects of the green spaces in the blocks. The thermal environmental effect of green space in 22 blocks in northwest Ganjingzi District was poor, specifically, in blocks No. 11, 14, 16, 17, 18, 19, 20, 21, 29,30, 32, 35, 36, 38, 43, 44, 45, 48, 59, 65, 70, and 77. One improvement method is to reduce the balance of green space, so that it forms a concentrated contiguous distribution.

Green spaces are not the only factor affecting the thermal environment [49]. In a number of recent studies, the contribution of urban blue and green spaces to urban cooling has been widely recognized, and more scholars have studied the comprehensive effects of blue and green spaces [20,50]. However, as this study area is a coastal city surrounded by the sea on three sides and has a temperate monsoon climate with maritime characteristics, the air humidity has hardly changed in 10 years, and the average annual relative humidity is 60–68%, so the influence of the humidity index is ignored. In addition, because its humidity conditions do not change much, green space is more significant to study compared with blue and green spaces. Furthermore, for the urban center, it is obviously more economical

and effective to achieve the cooling effect by adjusting the form and structural characteristics of green space, which has practical significance.

5.2. Limitations

There remain opportunities for improvement in the current research. First, the accuracy of green space and LST data differs, which limits the selection of the research scale to a certain extent and may also limit the correlation seen in other fractal indices at the block scale, except for the grid dimension. Second, there are regional differences in the development quality of green space and the characteristics of the urban thermal environment, and this study has only covered one case site of coastal cities (Dalian), and the comparison of multiple regions and similar cities requires continuous research. In addition, this study only discusses the thermal environmental effect of the fractal index of urban green space, and other factors will have interactive effects on the heat island effect. In the future, the comprehensive effects of various influencing factors will be analyzed.

6. Conclusions

Using high-resolution remote sensing data and a variety of spatial analysis models, an—for the first time—incorporating fractal theory and methods, we studied the thermal environment of the green structural index effect, evaluating 78 blocks in the study area to understand the spatial differences in quality of green space development. This study provides a new approach for formulating an optimization strategy for urban green space structures.

(1) At the block scale, the surface temperature in Dalian gradually increases from the coastal low-latitude areas to the inland high-latitude areas, forming a spatial distribution structure of "high in the central region and low in the surrounding region". At the block scale, the grid dimension of green space presents a "dual-core" spatial distribution structure, and both boundary dimensions present a "multi-core" spatial distribution structure.

(2) The LST of the block in Dalian had an obvious spatial effect, and the error impact of the regional thermal environment was stronger than the degree of spatial spillover from the thermal environment of its neighboring region. The driving direction and force of different green space indicators on the LST spatial pattern were different, and the influence of green space structural indicators was greater than that of green quality indicators. The neighborhood scale, based on the perimeter–scale model to estimate the urban green space boundary dimension, and the grid negative influence of the surface temperature, based on the perimeter–area model to estimate the urban green space dimension boundary on the surface temperature of the space difference pattern, had a positive influence. The influence of the green grid dimension on the spatial pattern of LST was the greatest.

(3) The spatial heterogeneity between the green space fractal index and LST in the Dalian block is significant and presents a centralized and contiguous spatial pattern. The spatial difference between the green space grid dimension and LST shows a trapezoidal structure that decreases from north to south. The "green space leading type" blocks have a poor cooling effect and poor green space development quality. These blocks are concentrated in the northwest of Ganjingzi District, totaling 22 blocks, which are key areas for future improvement. The block scale is the smallest unit that constitutes the planning, construction, and management of the territorial space. In the same block, the direction of urban planning, nature of land use, manner of human activity, and characteristics of the green space structure are homogeneous. It is scientific, practical, and instructive to evaluate the surface temperature, green space structure index, and their action mechanism on the block scale.

References

1. Mumtaz, F.; Li, J.; Liu, Q.; Tariq, A.; Arshad, A.; Dong, Y.; Zhao, J.; Bashir, B.; Zhang, H.; Gu, C.; et al. Impacts of Green Fraction Changes on Surface Temperature and Carbon Emissions: Comparison under Forestation and Urbanization Reshaping Scenarios. *Remote Sens.* **2023**, *15*, 859. [CrossRef]
2. Deilami, K.; Kamruzzaman, M.; Liu, Y. Urban heat island effect: A systematic review of spatio-temporal factors, data, methods, and mitigation measures. *Int. J. Appl. Earth Obs.* **2018**, *67*, 30–42. [CrossRef]
3. Feng, X.; Yu, J.; Xin, C.; Ye, T.; Wang, T.A.; Chen, H.; Zhang, X.; Zhang, L. Quantifying and Comparing the Cooling Effects of Three Different Morphologies of Urban Parks in Chengdu. *Land* **2023**, *12*, 451. [CrossRef]
4. Zheng, Y.; Li, W.; Fang, C.; Feng, B.; Zhong, Q.; Zhang, D. Investigating the Impact of Weather Conditions on Urban Heat Island Development in the Subtropical City of Hong Kong. *Atmosphere* **2023**, *14*, 257. [CrossRef]
5. Shu, Y.; Zou, K.; Li, G.; Yan, Q.; Zhang, S.; Zhang, W.; Liang, Y.; Xu, W. Evaluation of Urban Thermal Comfort and Its Relationship with Land Use/Land Cover Change: A Case Study of Three Urban Agglomerations, China. *Land* **2022**, *11*, 2140. [CrossRef]
6. Yang, J.; Wang, Y.; Xue, B.; Li, Y.; Xiao, X.; Xia, J.C.; He, B. Contribution of urban ventilation to the thermal environment and urban energy demand: Different climate background perspectives. *Sci. Total Environ.* **2021**, *795*, 148791. [CrossRef]
7. Qiu, X.; Kil, S.; Jo, H.; Park, C.; Song, W.; Choi, Y.E. Cooling Effect of Urban Blue and Green Spaces: A Case Study of Changsha, China. *Int. J. Environ. Res. Public Health* **2023**, *20*, 2613. [CrossRef]
8. Kong, D.; Zhang, Q.; Singh, V.P.; Shi, P. Seasonal Vegetation Response to Climate Change in The Northern Hemisphere (1982–2013). *Glob. Planet. Chang.* **2017**, *148*, 1–8. [CrossRef]
9. Zhang, B.; Xie, G.; Gao, J.; Yang, Y. The Cooling Effect of Urban Green Spaces As a Contribution to Energy-Saving and Emission-Reduction: A Case Study in Beijing, China. *Build. Environ.* **2014**, *76*, 37–43. [CrossRef]
10. Wang, L.; Zhang, S.; Yao, Y. The impacts of green landscape on urban thermal environment: A case study in Changchun city. *Geogr. Res.* **2014**, *33*, 2095–2104. [CrossRef]
11. Chen, S.; Haase, D.; Xue, B.; Wellmann, T.; Qureshi, S. Integrating Quantity and Quality to Assess Urban Green Space Improvement in the Compact City. *Land* **2021**, *10*, 1367. [CrossRef]
12. Kuang, W.; Dou, Y. Investigating the Patterns and Dynamics of Urban Green Space in China's 70 Major Cities Using Satellite Remote Sensing. *Remote Sens.* **2020**, *12*, 1929. [CrossRef]
13. Jiang, Y.; Huang, J.; Shi, T.; Wang, H. Interaction of Urban Rivers and Green Space Morphology to Mitigate the Urban Heat Island Effect: Case-Based Comparative Analysis. *Int. J. Environ. Res. Public Health* **2021**, *18*, 11404. [CrossRef] [PubMed]
14. Zhu, R.; Liu, Y.; Yan, B.; Zhang, X.; Yuan, L.; Wang, Y.; Pan, Y. Effects of district parameters, green space and building density on thermal comfort—A case study of Badaguan District in Qingdao. *Case Stud. Therm. Eng.* **2023**, *42*, 102705. [CrossRef]
15. Yin, S.; Peng, L.; Feng, N.; Wen, H.; Ling, Z.; Yang, X.; Dong, L. Spatial-temporal pattern in the cooling effect of a large urban forest and the factors driving it. *Build. Environ.* **2022**, *209*, 108676. [CrossRef]
16. Liu, W.; Jia, B.; Li, T.; Zhang, Q.; Ma, J. Correlation Analysis between Urban Green Space and Land Surface Temperature from the Perspective of Spatial Heterogeneity: A Case Study within the Sixth Ring Road of Beijing. *Sustainability* **2022**, *14*, 13492. [CrossRef]
17. Hou, J.; Wang, Y.; Zhou, D.; Gao, Z. Environmental Effects from Pocket Park Design According to District Planning Patterns—Cases from Xi'an, China. *Atmosphere* **2022**, *13*, 300. [CrossRef]
18. Manavvi, S.; Rajasekar, E. Assessing thermal comfort in urban squares in humid subtropical climate: A structural equation modelling approach. *Build. Environ.* **2023**, *229*, 109931. [CrossRef]

19. Kim, D.; Yu, J.; Yoon, J.; Jeon, S.; Son, S. Comparison of Accuracy of Surface Temperature Images from Unmanned Aerial Vehicle and Satellite for Precise Thermal Environment Monitoring of Urban Parks Using In Situ Data. *Remote Sens.* **2021**, *13*, 1977. [CrossRef]

20. Yan, L.; Jia, W.; Zhao, S. The Cooling Effect of Urban Green Spaces in Metacities: A Case Study of Beijing, China's Capital. *Remote Sens.* **2021**, *13*, 4601. [CrossRef]

21. Zhao, J.; Zhao, X.; Liang, S.; Wang, H.; Wu, D. Dynamic Cooling Effects of Permanent Urban Green Spaces in Beijing, China. *Remote Sens.* **2021**, *13*, 3282. [CrossRef]

22. Balany, F.; Muttil, N.; Muthukumaran, S.; Wong, M.S.; Ng, A.W.M. Studying the Effect of Blue-Green Infrastructure on Microclimate and Human Thermal Comfort in Melbourne’s Central Business District. *Sustainability* **2022**, *14*, 9057. [CrossRef]

23. Zhang, Y.; Hu, X.; Cao, X.; Liu, Z. Numerical Simulation of the Thermal Environment during Summer in Coastal Open Space and Research on Evaluating the Cooling Effect: A Case Study of May Fourth Square, Qingdao. *Sustainability* **2022**, *14*, 15126. [CrossRef]

24. Zhu, R.; Zhang, X.; Yang, L.; Liu, Y.; Cong, Y.; Gao, W. Correlation analysis of thermal comfort and physiological responses under different microclimates of urban park. *Case Stud. Therm. Eng.* **2022**, *34*, 102044. [CrossRef]

25. Liu, S.; Xu, M.; Zhao, J.; Sun, Y. Study on environmental effects of tree species in cities green space—Case on china. *J. Environ. Prot. Ecol.* **2022**, *23*, 40–48.

26. Zhang, Y.; Dai, M. Analysis of the Cooling and Humidification Effect of Multi-Layered Vegetation Communities in Urban Parks and Its Impact. *Atmosphere* **2022**, *13*, 2045. [CrossRef]

27. Su, Y.; Wu, J.; Zhang, C.; Wu, X.; Li, Q.; Liu, L.; Bi, C.; Zhang, H.; Lafortezza, R.; Chen, X. Estimating the cooling effect magnitude of urban vegetation in different climate zonesusing multi-source remote sensing. *Urban Clim.* **2022**, *43*, 101155. [CrossRef]

28. Yang, Y.; Hu, X.; Jin, X.; Yang, C.; Shu, D. Effects of three-dimensional green space distribution on cooling and humidification effect of plant community in summer: A case study of park green space in Huaihua City. *J. Hunan Agric. Univ. (Nat. Sci.)* **2022**, *48*, 181–189. [CrossRef]

29. Jiang, Y.; Jiang, S.; Shi, T. Comparative Study on the Cooling Effects of Green Space Patterns in Waterfront Build-Up Blocks: An Experience from Shanghai. *Int. J. Environ. Res. Public Health* **2020**, *17*, 8684. [CrossRef]

30. Zhang, Q.; Zhou, D.; Xu, D.; Cheng, J.; Rogora, A. Influencing factors of the thermal environment of urban green space. *Heliyon* **2022**, *8*, e11559. [CrossRef]

31. Pang, B.; Zhao, J.; Zhang, J.; Yang, L. How to plan urban green space in cold regions of China to achieve the best cooling efficiency. *Urban Ecosyst.* **2022**, *25*, 1181–1198. [CrossRef]

32. Chen, Y. *Study on the Temperature Effect of Urban Green Space Evolution in Fuzhou City*; Fujian Normal University: Fuzhou, China, 2020.

33. Ao, Y.; Wang, Z.; Zhao, Y.; Liang, L.; Zhang, M. Effect of green space landscape elements on temperature under different urbanization levels: A case study of Guanzhong Plain urban agglomeration. *Chin. J. Ecol.* **2022**, 1–15.

34. Lin, B.; Yang, X.; Zhang, Y.; Wu, L.; Wang, Y.; Guo, G. Cooling effect of urban green space of Guangzhou core area. *Ecol. Sci.* **2021**, *40*, 26–34. [CrossRef]

35. Sun, X.; Tan, X.; Chen, K.; Song, S.; Zhu, X.; Hou, D. Quantifying landscape-metrics impacts on urban green-spaces and water-bodies cooling effect: The study of Nanjing, China. *Urban For. Urban Green.* **2020**, *55*, 126838. [CrossRef]

36. Luecke, G.R. GREENSPACE: Virtual Reality Interface for Combine Operator Training. *Presence* **2012**, *21*, 245–253. [CrossRef]

37. Soares, M.M.; Maia, E.G.; Claro, R.M. Availability of public open space and the practice of leisure-time physical activity among the Brazilian adult population. *Int. J. Public Health* **2020**, *65*, 1467. [CrossRef]

38. Barbosa, O.; Tratalos, J.A.; Armsworth, P.R.; Davies, R.G.; Fuller, R.A.; Johnson, P.; Gaston, K.J. Who benefits from access to green space? A case study from Sheffield, UK. *Landsc. Urban Plan.* **2007**, *83*, 187–195. [CrossRef]

39. Luo, Y.; Peng, W.; Dong, Y.; Luo, Y.; Zhang, D. Geographical exploration of the spatial pattern of the surface temperature and its influencing factors in western Sichuan Plateau: A case of Xichang City. *Arid. Land Geogr.* **2020**, *43*, 738–749. [CrossRef]

40. Jinxin, H.E.; Sun, H.; Wenqing, L.I.; Zheng, B.; Jiang, T. Land Surface Temperature Retrieval in Eastern Liaoning Geothermal Area Based on Thermal Infrared Remote Sensing Data. *J. Jilin Univ. (Inf. Sci. Ed.)* **2018**, *36*, 62–68. [CrossRef]

41. Tan, Z.; Minghua, Z.; Karnieli, A.; Berliner, P. A single window algorithm for land surface temperature calculation using Landsat TM6 data. *Acta Geogr. Sin.* **2001**, *1*, 456–466. [CrossRef]

42. Gong, Y.; Li, X.; Cong, X.; Liu, H. Research on the Complexity of Forms and Structures of Urban Green Spaces Based on Fractal Models. *Complexity* **2020**, *2020*, 4213412. [CrossRef]

43. Zhou, Y.; Chen, L.; Liu, T. Application of fractal theory to sediment research. *J. Sediment Res.* **2012**, 73–80. [CrossRef]

44. Liu, J.; Chen, Y. Fractal dimensions of spatial structure of an urban system and the methods of their determination. *Geogr. Res.* **1999**, *2*, 60–67.

45. Liu, J.; Zhang, L.; Ji, Y.; Zhang, Q. Spatial-Temporal Evolution Analysis of Urban Green Space System Based on Fractal Model: A Case Study of Downtown Shanghai. *Mod. Urban Res.* **2019**, *10*, 12–19.

46. Chen, K.; Gong, J.; Chen, X.; Li, T. The Pattern Relationship Research of Green Space and Surface Temperature in Guangzhou City. *Ecol. Environ. Sci.* **2016**, *25*, 842–849. [CrossRef]

47. Xiao, Z. Spatial Effect of Population-Economic Distribution Consistency in China. *Popul. Res.* **2013**, *37*, 42–52.

48. Zhou, C.; Ye, C. Progress on studies of urban spatial structure in China. *Prog. Geogr.* **2013**, *32*, 1030–1038. [CrossRef]

49. Zhang, Y.; Wang, Y.; Ding, N. Spatial Effects of Landscape Patterns of Urban Patches with Different Vegetation Fractions on Urban Thermal Environment. *Remote Sens.* **2022**, *14*, 5684. [CrossRef]

50. Chen, L.; Wang, X.; Cai, X.; Yang, C.; Lu, X. Combined Effects of Artificial Surface and Urban Blue-Green Space on Land Surface Temperature in 28 Major Cities in China. *Remote Sens.* **2022**, *14*, 448. [CrossRef]